Thermal Degradation of Poly(Allyl Methacrylate) by Mass Spectroscopy and TGA

Tuğba Kantav Vardareli[a]; Selda Keskn[a]; Al Usanmaz[a]

[a] Department of Chemistry and Polymer Science and Technology, Middle East Technical University, Ankara, Turkey

PLEASE SCROLL DOWN FOR ARTICLE

Thermal Degradation of Poly(Allyl Methacrylate) by Mass Spectroscopy and TGA

TUĞBA KANTAV VARDARELİ, SELDA KESKİN,
AND ALİ USANMAZ

Department of Chemistry and Polymer Science and Technology,
Middle East Technical University, Ankara, Turkey

Allyl methacrylate, AMA was polymerized in CCl₄ solution by α,α′-azoisobutyronitrile at 50°C. The thermal degradation mechanism of PAMA was characterized by MS, TGA-FT-IR and FT-IR-ATR methods. The mass spectrum and TGA thermogram showed two stage degradation. The first stage of degradation was mostly linkage type degradation for the fragmentation of pendant allyl groups at 225–350°C. In the second stage, at 395–515°C, the degradation is random scission and depolymerization types. This was also supported by direct thermal pyrolysis of polymer under vacuum. The degradation fragments of MS and TGA were in agreement. In the degradation process, monomer degraded further to CO, CO₂, allyl and ether groups. No strong monomer peak was observed in mass spectrum.

Keywords allyl methacrylate, mass spectroscopy, TGA, thermal degradation, FT-IR

Introduction

The polymerization of allyl methacrylate, AMA by different polymerization methods have been reported (1–14). In most of the published works, the possible cyclopolymerization to give lactones are discussed. The solubility of polymer is attributed to the linear nature of the polymer chain. Thus, the insolubility of polymer is suggested to be due to the cross-linking with allyl groups. However, in our previous work (15) it was shown that the insolubility of PAMA is mostly related to the molecular weight but partially to crosslinking. Even at very high conversions, only 1–2% of allyl groups are involved in cyclization and/or crosslinking. This was also reported by bromination of pendant allyl groups in linear polymer (1, 2). The degradation of PAMA and its copolymer were studied by Zulfigar et al. (12–14) using TGA, TVA, DTA and GC-MS methods. They have collected the degradation fragments and characterize them by FT-IR after separation of fragments by condensation. The main pyrolysis products were related to the nature of polymer chain.

In the previous work (15), the polymerization mechanism of AMA under different conditions was studied. The polymer chain structure was investigated by different methods such as FT-IR, NMR, DSC, TGA and ESCA. In this study, thermal degradation of PAMA was carried out by MS, TGA *in situ* FT-IR and thermal pyrolysis residual by FT-IR-ATR. This should give us the detailed chain structure and the thermal properties of the polymer.

Experimental

Materials

Allyl methacrylate, AMA (Aldrich) was purified by distillation. α,α'-Azoisobutyronitrile, AIBN (Merck), carbontetrachloride (Merck), methanol (Riedel-de Haën) and toluene (Merck) were all spectroscopic grade and used without further purification.

Polymer Characterization

The FT-IR spectra were taken on a Bruker Vertex 70 ATR-FT-IR Spectrometer using KBr pellets. TGA *in situ* FT-IR thermogram was taken on a Perkin-Elmer Pyris 1 TGA and spectrum 1 FT-IR Spectrometer under nitrogen gas atmosphere in a temperature range of 30–800°C with a heating rate of 5°C/min. The mass spectrometer was a Balzers QMG 311 quadrupole with an electron impact of 70 eV. The scan rate of heating was 10°C/min starting at 25°C. The instrumental control and data acquisition was carried out by computer.

Procedure

For the polymerization, 2 ml (15 mmol) AMA, 5 mg (0.03 mmol) AIBN, and 4 ml CCl$_4$ were placed in a Pyrex tube, which was degassed via three freeze-pump-thaw cycles on a high vacuum system. The tube under vacuum was sealed by flame and placed in a constant temperature oil bath at 50°C for the desired period. It was then broken open, the polymer precipitated by excess methanol, filtered and dried under vacuum to constant weight. The soluble fraction was extracted with toluene. The results for the kinetic and mechanism of polymerization are given in another publication (15).

For thermal pyrolysis, the polymer sample was heated at (a) 280 and (b) 350°C in an evacuated test tube. The FT-IR of residual polymer, after removal of volatile degraded fragments, was recorded.

Results and Discussion

The thermal degradation of PAMA was carried out by direct thermal pyrolysis, MS and TGA *in situ* FT-IR. The FT-IR spectrum of residual samples of PAMA after pyrolysis at (a) 280 and (b) 350°C are given in Figure 1. The allyl peaks (Figure 1a) observed at 3084.5, 1648.1 and 931.9 cm^{-1} almost disappeared after thermal treatment at 350°C as shown in Figure 1b. Thus, at about 350°C, the linkage degradation of side groups in the polymer chain is maximized with the possible formation of anhydride and end group cyclization to lactones (Scheme 3). The details of fragmentation are obtained from mass spectra and TGA thermogram.
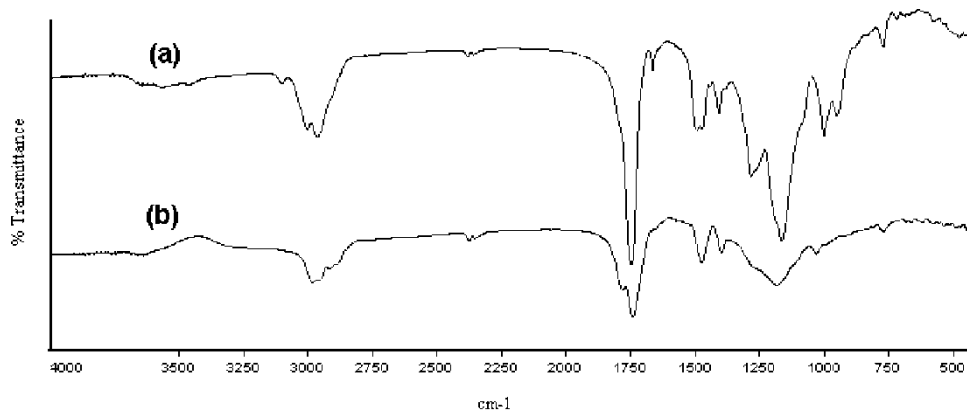
Figure 1. The FT-IR spectrum of residual samples of PAMA after pyrolysis at (a) 280°C and (b) 350°C.

Mass Spectral Investigation

The mass spectra of (a) insoluble (b) soluble PAMA are given in Figure 2. The fragmentation in each of the thermograms show two regions at about 225–350°C and 395–515°C.

Figure 2. Mass thermogram scanning of (a) insoluble and (b) soluble PAMA.

Figure 3. Fragments of insoluble PAMA obtained at (a) 142°C, (b) 335°C and, (c) 442°C

Table 1
The relative abundances of the peaks and their fragments for insoluble PAMA fraction

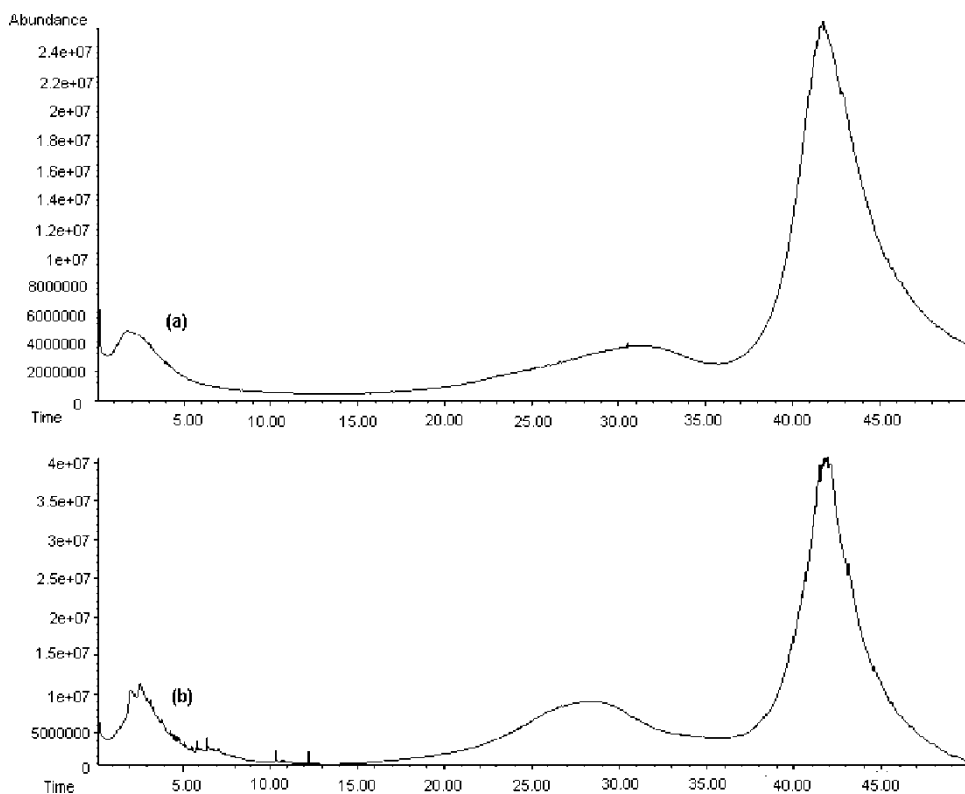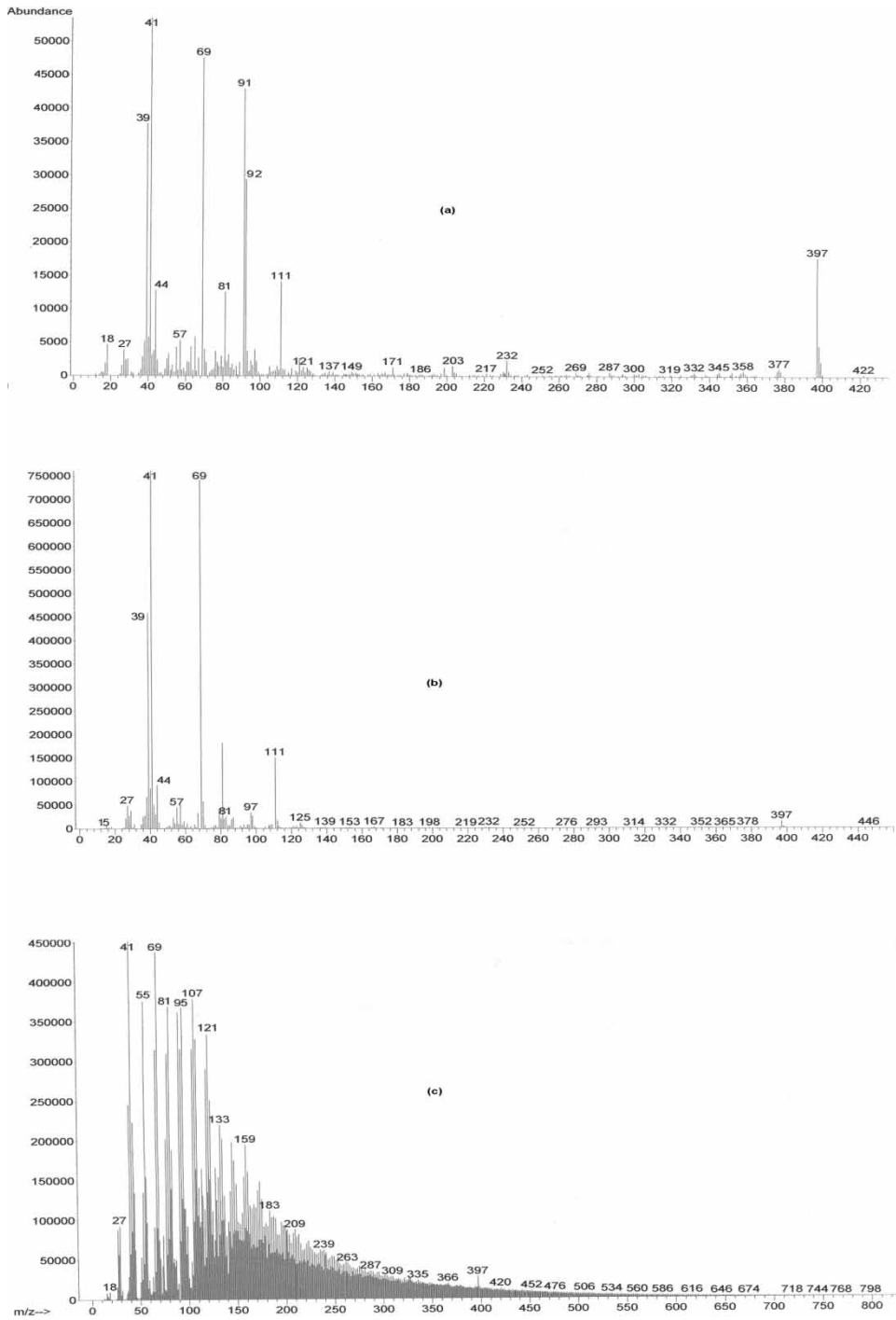| m/z | 142°C | | | 335°C | | | 442°C | | |
	I/I_0	Fragments		I/I_0	Fragments		I/I_0	Fragments
15	0.11	CH_3		1.05	CH_3		1.05	CH_3
18	0.65	H_2O		0.57	H_2O		1.12	H_2O
26	0.24	CN, C_2H_2		2.93	CN, C_2H_2		2.15	CN, C_2H_2
27	0.49	C_2H_3		6.48	C_2H_3		11.64	C_2H_3
28	0.33	CO		3.70	CO		7.46	CO
31	0.08	CH_3O		1.39	CH_3O		1.46	CH_3O
35	0.07	Cl		0.96	Cl		0.33	Cl
39	4.80	C_3H_3		60.26	C_3H_3		32.36	C_3H_3
41	7.07	C_3H_5		100	C_3H_5		58.43	C_3H_5
44	1.78	CO_2		12.31	CO_2		17.39	CO_2
45	0.32	CHO_2		1.77	CHO_2		8.11	CHO_2
55	0.56	C_3H_3O		6.21	C_3H_3O		48.86	C_3H_3O
57	0.70	C_3H_5O		7.69	C_3H_5O		12.74	C_3H_5O
69	6.14	C_4H_5O		97.79	C_4H_5O		56.46	C_4H_5O
77	0.30	C_6H_5		1.01	C_6H_5		26.19	C_6H_5
81	1.53	C_4HO_2		24.42	C_4HO_2		48.31	C_4HO_2
87	0.22	$C_4H_7O_2$		2.76	$C_4H_7O_2$		6.25	$C_4H_7O_2$
91	5.84	C_6H_5N		0.87	C_6H_5N		47.72	C_6H_5N
95	0.25	$C_5H_3O_2$		1.29	$C_5H_3O_2$		48.08	$C_5H_3O_2$
97	0.49	$C_5H_5O_2$		4.61	$C_5H_5O_2$		15.65	$C_5H_5O_2$
107	0.06	$C_6H_3O_2$		0.95	$C_6H_3O_2$		48.82	$C_6H_3O_2$
111	1.87	$C_6H_7O_2$		19.94	$C_6H_7O_2$		18.50	$C_6H_7O_2$
117	0.15	CCl_3		0.17	CCl_3		15.21	CCl_3
121	0.25	$C_7H_5O_2$		0.71	$C_7H_5O_2$		43.47	$C_7H_5O_2$
123	0.17	$C_7H_7O_2$		0.65	$C_7H_7O_2$		33.40	$C_7H_7O_2$
125	0.19	$C_7H_9O_2$		1.49	$C_7H_9O_2$		14.29	$C_7H_9O_2$
126	0.10	$C_7H_{10}O_2$ (AMA)		1.09	$C_7H_{10}O_2$ (AMA)		6.87	$C_7H_{10}O_2$ (AMA)
133	0.04	$C_8H_5O_2$		0.16	$C_8H_5O_2$		28.70	$C_8H_5O_2$
137	0.08	$C_6H_5O_3$		0.22	$C_6H_5O_3$		16.65	$C_6H_5O_3$
139	0.08	$C_6H_7O_3$		0.41	$C_6H_7O_3$		10.22	$C_6H_7O_3$
149	0.12	$C_9H_5O_2$		0.16	$C_9H_5O_2$		19.59	$C_9H_5O_2$
153	0.06	$C_9H_9O_2$		0.32	$C_9H_9O_2$		12.06	$C_9H_9O_2$
159	0.04	$C_7H_{11}O_4$		0.08	$C_7H_{11}O_4$		25.63	$C_7H_{11}O_4$
167	0.07	$C_8H_7O_4$		0.06	$C_8H_7O_4$		15.90	$C_8H_7O_4$
171	0.22	$C_9H_{17}O_2N$, $C_8H_{11}O_4$		0.25	$C_9H_{17}O_2N$, $C_8H_{11}O_4$		18.41	$C_9H_{17}O_2N$, $C_8H_{11}O_4$
185	0.03	$C_9H_{13}O_4$		0.05	$C_9H_{13}O_4$		13.85	$C_9H_{13}O_4$
195	—	$C_{11}H_{15}O_3$		0.04	$C_{11}H_{15}O_3$		12.45	$C_{11}H_{15}O_3$
203	0.24	$C_{12}H_{13}O_2N$		0.21	$C_{12}H_{13}O_2N$		10.58	$C_{12}H_{13}O_2N$
209	0.03	$C_{11}H_{13}O_4$		0.04	$C_{11}H_{13}O_4$		11.57	$C_{11}H_{13}O_4$

(*continued*)

Table 1
Continued

m/z	142°C			335°C		442°C	
	I/I_0	Fragments	I/I_0	Fragments	I/I_0	Fragments
219	0.03	$C_{12}H_{11}O_4$	0.03	$C_{12}H_{11}O_4$	8.43	$C_{12}H_{11}O_4$
233	0.06	$C_{14}H_{19}O_2N$, $C_{14}H_{16}O_4$	0.07	$C_{14}H_{19}O_2N$, $C_{14}H_{16}O_4$	7.76	$C_{14}H_{19}O_2N$, $C_{14}H_{16}O_4$
252	0.02	$C_{14}H_{20}O_4$ (dimer)	0.03	$C_{14}H_{19}O_4$ (dimer)	6.96	$C_{14}H_{19}O_4$ (dimer)
269	0.10	$C_{14}H_{21}O_5$	0.09	$C_{14}H_{21}O_5$	5.18	$C_{14}H_{21}O_5$
276	0.09	$C_{15}H_{16}O_6$	0.09	$C_{15}H_{16}O_6$	4.16	$C_{15}H_{16}O_6$
287	0.07	$C_{14}H_{23}O_6$	0.07	$C_{14}H_{23}O_6$	4.50	$C_{14}H_{23}O_6$
293	0.03	$C_{17}H_{25}O_5$	0.03	$C_{17}H_{25}O_5$	4.33	$C_{17}H_{25}O_5$
301	0.02	$C_{15}H_{25}O_6$	0.05	$C_{15}H_{25}O_6$	3.96	$C_{15}H_{25}O_6$
319	0.05	$C_{18}H_{23}O_5$	0.04	$C_{18}H_{23}O_5$	3.02	$C_{18}H_{23}O_5$
332	0.10	$C_{18}H_{20}O_6$	0.10	$C_{18}H_{20}O_6$	2.43	$C_{18}H_{20}O_6$
345	0.08	$C_{19}H_{21}O_6$	0.09	$C_{19}H_{21}O_6$	2.44	$C_{19}H_{21}O_6$
352	0.11	$C_{19}H_{28}O_6$	0.09	$C_{19}H_{28}O_6$	2.26	$C_{19}H_{28}O_6$
358	0.07	$C_{20}H_{22}O_6$	0.09	$C_{20}H_{22}O_6$	2.22	$C_{20}H_{22}O_6$
365	0.03	$C_{20}H_{29}O_6$	0.03	$C_{20}H_{29}O_6$	2.27	$C_{20}H_{29}O_6$
377	0.13	$C_{15}H_{14}Cl_3O_4N$	0.10	$C_{15}H_{14}Cl_3O_4N$	2.07	$C_{15}H_{14}Cl_3O_4N$
378	0.10	$C_{21}H_{30}O_6$ (trimer)	0.09	$C_{21}H_{30}O_6$ (trimer)	2.04	$C_{21}H_{30}O_6$ (trimer)
397	2.54	$C_{16}H_{22}Cl_3O_4N$	1.97	$C_{16}H_{22}Cl_3O_4N$	3.53	$C_{16}H_{22}Cl_3O_4N$
422	0.02	$C_{22}H_{30}O_8$ (tetramer)	—	$C_{22}H_{30}O_8$ (tetramer)	1.40	$C_{22}H_{30}O_8$ (tetramer)
616	—	$C_{34}H_{48}O_{10}$ (pentamer)	—	$C_{34}H_{48}O_{10}$ (pentamer)	0.25	$C_{34}H_{48}O_{10}$ (pentamer)
718	—	$C_{40}H_{46}O_{12}$ (hexamer)	—	$C_{40}H_{46}O_{12}$ (hexamer)	0.07	$C_{40}H_{46}O_{12}$ (hexamer)
798	—	$C_{43}H_{58}O_{14}$ (heptamer)	—	$C_{43}H_{58}O_{14}$ (heptamer)	0.04	$C_{43}H_{58}O_{14}$ (heptamer)

The first peak is broader and mostly due to the linkage breaking of pendant allyl groups. The intensity of the second peak is higher, which shows the main polymer chain scissoring and/or depolymerization followed by fragmentation at this temperature range. The small difference between the two thermograms (Figures 2a and 2b) are in peak shape and peak positions. Especially, the first peak area in the soluble PAMA (Figure 2b) is larger because oligomers and cyclic adducts are extracted into this fraction. They are degraded mostly at this temperature range. The second peak area (Figure 2a) is larger and extends to higher temperatures for insoluble PAMA due to some oligomers and cyclic adducts degraded at this stage. The broad peak at 25–125°C in both spectra corresponds to the impurities (residual monomer and solvent, etc).
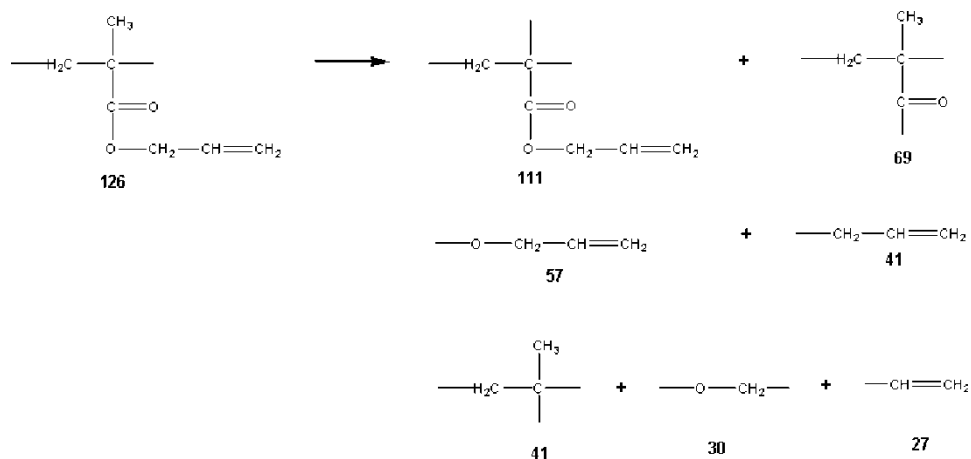
Scheme 1. Degradation of allyl group of PAMA.

The detailed fragmentation at (a) 142, (b) 335 and (c) 442°C for insoluble PAMA is given in Figure 3. The relative abundances of the peaks and their fragments are given in Table 1. In Figure 3a, the temperature is 142°C (11.7 min in Figure 2a). There is no apparent degradation peak at 11.7 min. Therefore, the peaks observed (Figure 3a) are due to the fragmentation of residual monomer and other possible oligomers that formed during the polymerization. The monomer peak at 126 is very weak in the spectrum showing the predominant monomer fragmentation. The residual monomer is degraded to give the main peaks at 27, 30, 41, 57, 69, and 111 (Table 1), similar to the reported fragments by Zulfigar et al. (12–14). The fragmentation of monomer is shown in Scheme 1.

The peak at 397 corresponds to a cyclic oligomer containing AIBN and CCl$_4$ fragments as in Scheme 2. The observed weak peaks at 398, 399 and 400 are in agreement to the isotopes of Cl. The fragmentation of this product gives weak peaks at 377, 233, 203 and 171 (Table 1). The presence of Cl and N is also shown (15) in the ESCA spectrum of PAMA.

The thermal fragmentation at 335°C is given in Figure 3b and the results are tabulated in Table 1. The basic thermal behavior of the polymer at this stage of degradation is mainly formation of anhydride and end group cyclization as also shown by FT-IR spectrum

$m/z = 397$
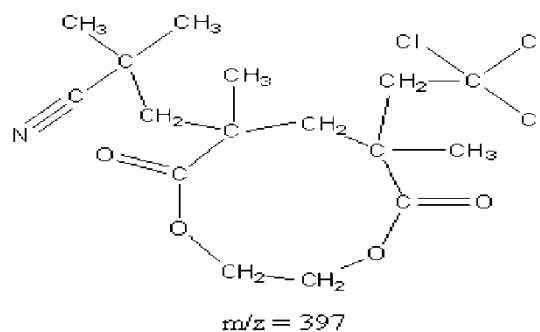
**Scheme 2.** Cylic oligomer formed during polymerization of AMA.

(Figure 1) of residual sample after direct thermal pyrolysis. Therefore, the anhydride formation and/or cyclization to lactones are shown in Scheme 3.

The fragmentation at 442°C for insoluble PAMA is similar to that at 335°C, with increasing number of fragments. These are mostly main chain degradation products.

The mass spectrum for the soluble fraction of PAMA is given in Figure 2b. The observed m/z at (a) 309 (b) 405 and (c) 441°C is given in Figure 4 and the m/z data at three different temperatures are tabulated in Table 2. The fragment abundance is maximum at 335°C for the insoluble fraction of PAMA (Figure 3b) and that of the soluble fraction is 309°C (Figure 4a). The two thermograms are quite similar with changes in the relative abundance of fragments.

TGA Investigation

The TGA thermogram for the insoluble fraction of PAMA was reported before (15) and for soluble fraction, it is given in Figure 5 in the temperature range of 30–800°C. The degradation of insoluble fraction showed two-stage degradation (15) with second stage peak being more intense. The thermogram for soluble fraction showed three degradation stages. The reduction in the weight of polymer started above 100°C became sharper after 200°C and showed a break in the change of slope at 300°C. The slope of the thermogram curve between 200–300°C is sharp indicating the
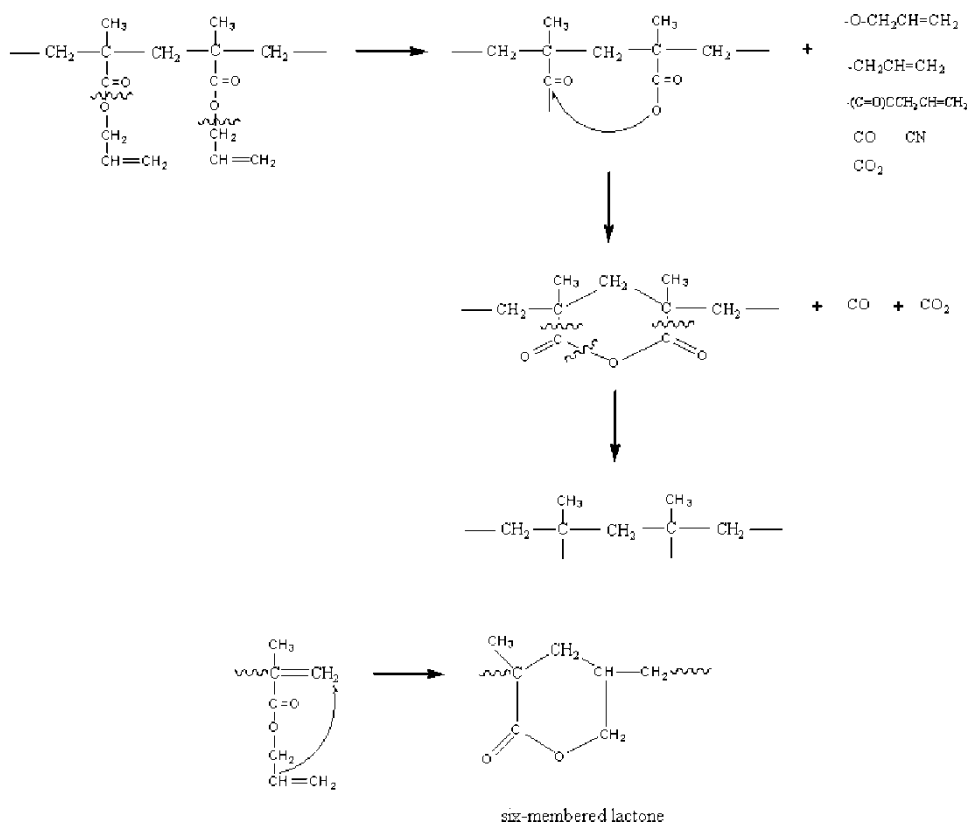
Scheme 3. Degradation of PAMA with formation of anhydride and lactons.

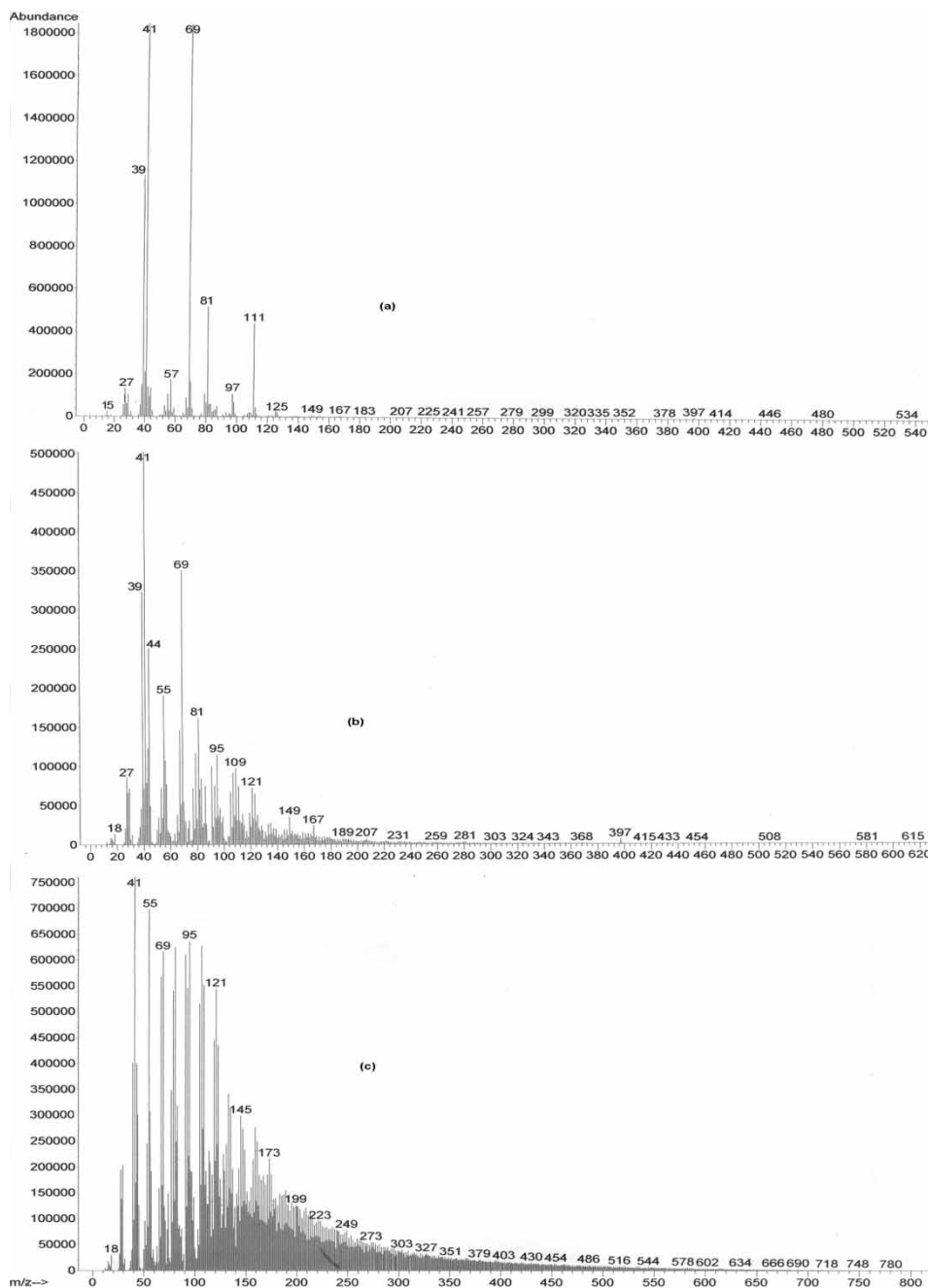**Figure 4.** Fragments of soluble PAMA obtained at (a) 309°C (b) 405°C and (c) 441°C

depolymerization mechanism. However, it was shown from the mass spectrum that the monomer does not come out as a fragment, but is fragmented into its components. Thus, in TGA analysis, the polymer is depolymerized to give monomer which is immediately degraded to its fragments. They are observed in FT-IR (Figure 6)

Table 2
The relative abundances of the peaks and their fragments for soluble PAMA fraction

	309°C		405°C		441°C	
m/z	I/I_0	Fragments	I/I_0	Fragments	I/I_0	Fragments
15	1.21	CH_3	0.57	CH_3	0.98	CH_3
18	0.33	H_2O	0.72	H_2O	1.68	H_2O
26	2.97	CN, C_2H_2	1.17	CN, C_2H_2	1.61	CN, C_2H_2
27	6.94	C_2H_3	4.56	C_2H_3	10.25	C_2H_3
28	3.28	CO	3.77	CO	7.09	CO
29	5.46	C_2H_5, CHO	4.12	C_2H_5, CHO	10.97	C_2H_5, CHO
31	1.29	CH_3O	0.59	CH_3O	1.15	CH_3O
35	0.10	Cl	0.13	Cl	0.04	Cl
39	60.63	C_3H_3	17.36	C_3H_3	21.48	C_3H_3
41	100	C_3H_5	27.25	C_3H_5	40.91	C_3H_5
44	6.93	CO_2	13.78	CO_2	15.84	CO_2
45	1.45	CHO_2	2.59	CHO_2	6.56	CHO_2
55	5.94	C_3H_3O	10.49	C_3H_3O	38.24	C_3H_3O
57	9.41	C_3H_5O	4.12	C_3H_5O	10.71	C_3H_5O
69	99.09	C_4H_5O	19.47	C_4H_5O	33.03	C_4H_5O
77	0.85	C_6H_5	3.53	C_6H_5	18.66	C_6H_5
81	27.22	C_4HO_2	8.78	C_4HO_2	33.65	C_4HO_2
87	3.14	$C_4H_7O_2$	1.49	$C_4H_7O_2$	4.32	$C_4H_7O_2$
91	0.69	C_6H_5N	5.39	C_6H_5N	33.60	C_6H_5N
95	1.10	$C_5H_3O_2$	6.10	$C_5H_3O_2$	34.00	$C_5H_3O_2$
97	5.62	$C_5H_5O_2$	2.54	$C_5H_5O_2$	10.67	$C_5H_5O_2$
107	0.82	$C_6H_3O_2$	5.13	$C_6H_3O_2$	34.28	$C_6H_3O_2$
111	23.35	$C_6H_7O_2$	4.00	$C_6H_7O_2$	10.36	$C_6H_7O_2$
117	0.19	CCl_3	1.07	CCl_3	10.26	CCl_3
121	0.52	$C_7H_5O_2$	3.75	$C_7H_5O_2$	29.92	$C_7H_5O_2$
123	0.50	$C_7H_7O_2$	3.50	$C_7H_7O_2$	23.58	$C_7H_7O_2$
125	1.66	$C_7H_9O_2$	1.95	$C_7H_9O_2$	9.17	$C_7H_9O_2$
126	1.15	$C_7H_{10}O_2$ (AMA)	1.18	$C_7H_{10}O_2$ (AMA)	4.38	$C_7H_{10}O_2$ (AMA)
133	0.30	$C_8H_5O_2$	1.41	$C_8H_5O_2$	18.31	$C_8H_5O_2$
137	0.29	$C_6H_5O_3$	1.07	$C_6H_5O_3$	10.66	$C_6H_5O_3$
139	0.28	$C_6H_7O_3$	1.05	$C_6H_7O_3$	6.67	$C_6H_7O_3$
149	0.62	$C_9H_5O_2$	1.71	$C_9H_5O_2$	12.62	$C_9H_5O_2$
153	0.21	$C_9H_9O_2$	0.75	$C_9H_9O_2$	7.34	$C_9H_9O_2$
159	0.06	$C_7H_{11}O_4$	0.76	$C_7H_{11}O_4$	15.64	$C_7H_{11}O_4$
167	0.31	$C_8H_7O_4$	1.42	$C_8H_7O_4$	10.20	$C_8H_7O_4$
171	0.11	$C_9H_{17}O_2N$, $C_8H_{11}O_4$	0.46	$C_9H_{17}O_2N$, $C_8H_{11}O_4$	10.27	$C_9H_{17}O_2N$, $C_8H_{11}O_4$
185	0.16	$C_9H_{13}O_4$	0.39	$C_9H_{13}O_4$	7.85	$C_9H_{13}O_4$
195	0.11	$C_{11}H_{15}O_3$	0.40	$C_{11}H_{15}O_3$	7.44	$C_{11}H_{15}O_3$
203	0.06	$C_{12}H_{13}O_2N$	0.35	$C_{12}H_{13}O_2N$	6.71	$C_{12}H_{13}O_2N$

Table 2
Continued

m/z	309°C			405°C			441°C		
	I/I_0	Fragments	I/I_0	Fragments	I/I_0	Fragments
209	0.09	$C_{11}H_{13}O_4$	0.29	$C_{11}H_{13}O_4$	6.78	$C_{11}H_{13}O_4$
219	0.03	$C_{12}H_{11}O_4$	0.23	$C_{12}H_{11}O_4$	5.29	$C_{12}H_{11}O_4$
233	0.05	$C_{14}H_{19}O_2N,$ $C_{14}H_{16}O_4$	0.15	$C_{14}H_{19}O_2N,$ $C_{14}H_{16}O_4$	4.40	$C_{14}H_{19}O_2N,$ $C_{14}H_{16}O_4$
252	0.04	$C_{14}H_{20}O_4$ (dimer)	0.09	$C_{14}H_{19}O_4$ (dimer)	2.57	$C_{14}H_{19}O_4$ (dimer)
269	0.03	$C_{14}H_{21}O_5$	0.07	$C_{14}H_{21}O_5$	3.15	$C_{14}H_{21}O_5$
287	0.04	$C_{14}H_{23}O_6$	0.05	$C_{14}H_{23}O_6$	2.60	$C_{14}H_{23}O_6$
301	0.02	$C_{15}H_{25}O_6$	0.04	$C_{15}H_{25}O_6$	2.24	$C_{15}H_{25}O_6$
319	0.01	$C_{18}H_{23}O_5$	0.06	$C_{18}H_{23}O_5$	1.75	$C_{18}H_{23}O_5$
332	0.04	$C_{18}H_{20}O_6$	0.06	$C_{18}H_{20}O_6$	1.39	$C_{18}H_{20}O_6$
345	0.02	$C_{19}H_{21}O_6$	0.04	$C_{19}H_{21}O_6$	1.39	$C_{19}H_{21}O_6$
352	0.04	$C_{19}H_{28}O_6$	0.02	$C_{19}H_{28}O_6$	1.15	$C_{19}H_{28}O_6$
358	0.01	$C_{20}H_{22}O_6$	0.03	$C_{20}H_{22}O_6$	1.24	$C_{20}H_{22}O_6$
365	0.02	$C_{20}H_{29}O_6$	0.03	$C_{20}H_{29}O_6$	1.26	$C_{20}H_{29}O_6$
378	0.01	$C_{21}H_{30}O_6$ (trimer)	0.02	$C_{21}H_{30}O_6$ (trimer)	1.11	$C_{21}H_{30}O_6$ (trimer)
397	0.26	$C_{16}H_{22}Cl_3$ O_4N	0.24	$C_{16}H_{22}Cl_3$ O_4N	1.08	$C_{16}H_{22}Cl_3$ O_4N
422	—	$C_{22}H_{30}O_8$ (tetramer)	—	$C_{22}H_{30}O_8$ (tetramer)	0.98	$C_{22}H_{30}O_8$ (tetramer)
624	—	$C_{35}H_{44}O_{10}$ (pentamer)	0.01	$C_{35}H_{44}O_{10}$ (pentamer)	0.04	$C_{35}H_{44}O_{10}$ (pentamer)
748	—	$C_{42}H_{52}O_{12}$ (hexamer)	—	$C_{42}H_{52}O_{12}$ (hexamer)	0.04	$C_{42}H_{52}O_{12}$ (hexamer)
800	—	$C_{43}H_{60}O_{14}$ (heptamer)	—	$C_{43}H_{60}O_{14}$ (heptamer)	0.01	$C_{43}H_{60}O_{14}$ (heptamer)

connected to TGA. At 225°C, FT-IR spectrum (Figure 6a) showed the fragments corresponding to $-CH_2$ at 2900–3000 cm^{-1}; allyl groups at 3084.5, 1648.1 and 931.9 cm^{-1}; CO, CO_2 and CN at 2200–2300 cm^{-1}; carbonyl corresponding to ester anhydride, and lactones at 1720–1850 cm^{-1}; ether and ester at 1100–1300 cm^{-1}. Further temperature treatment (Figure 6b, 390°C) gives similar fragmentation with increase of peak intensity for CO, CO_2 and CN and peak broadening of carbonyl group. This can be due to the anhydride and lactones formation which fragmented according to Scheme 3 to give more CO and CO_2. At 580°C (Figure 6c) the emission of CO and CO_2 is almost completed and the most important fragments are ether or ester type. At this stage, the emissions of OH and NH groups are also noticeable and the complete fragmentation reaches to about 97%. Therefore, the degradation is almost completed at about 600°C.
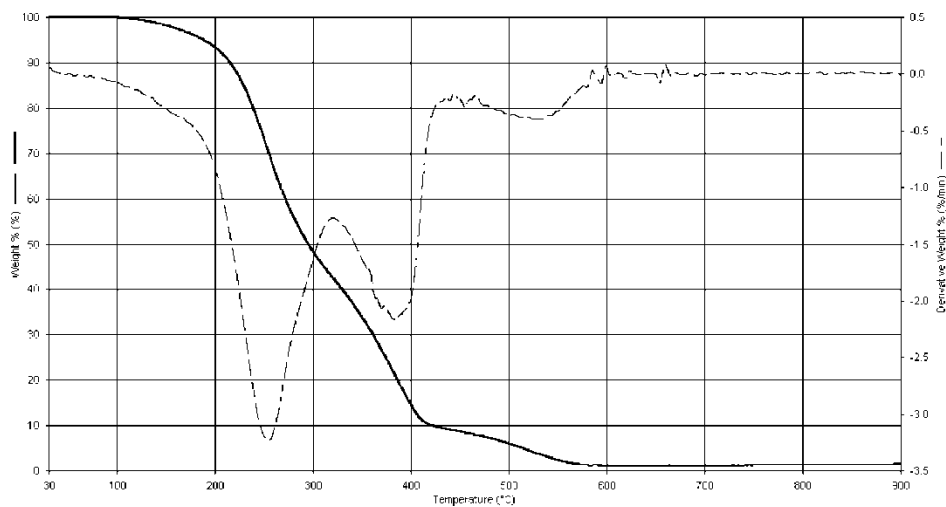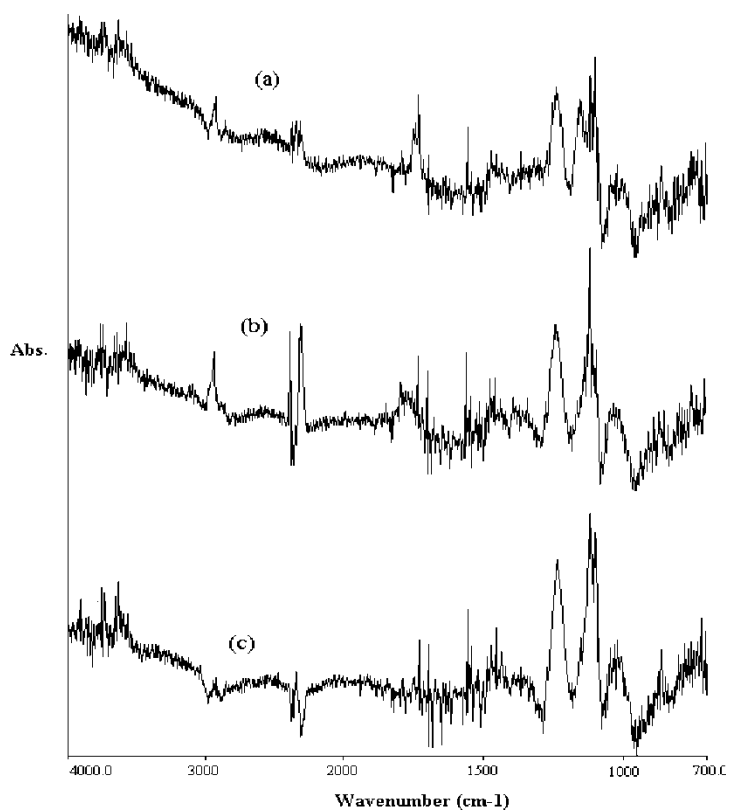
Figure 5. TGA thermogram of soluble fraction of PAMA.

Figure 6. FT-IR spectrum of degraded PAMA fragments from TGA at (a) 225°C, (b) 390°C, and (c) 580°C.

Conclusions

The degradation of PAMA was studied by MS and TGA. The mechanism of degradation was clarified by analysis of fragments degraded from polymer at different temperatures. Degradation of the polymer chain is generally a depolymerization type. However, the depolymerized monomer is readily degraded further to give its fragments. Generally, in mass spectrum the monomer peak is the main peak for the polymer degradation. In the case of PAMA, the monomer peak is very weak in the spectrum. The main fragmentation is the pendant allyl group breakage. This also indicates that the cyclopolymerization as suggested in the literature (4, 5, 8) has not taken place. Under proper conditions, the pendant allyl groups can rearrange to give anhydrides or end group cyclization giving lactones. The anhydride formation is predominant at around 300°C.

References

1. Cohen, S.G. and Sparrow, D.B. (1948) *J. Polym. Sci.*, 3: 693–703.
2. D'Alelio, G.F. and Hoffend, T.R. (1967) *J. Polym. Sci.: Part A–1*, 5: 323–337.
3. Zhang, H. and Ruckenstein, E. (1997) *J. Polym. Sci.: Part A: Polym. Chem.*, 35: 2901–2906.
4. Higgins, J.P.J. and Weale, K.E. (1968) *J. Polym. Sci.: Part A–1*, 6: 3007–3013.
5. Matsumoto, A., Ishido, H., and Oiwa, M. (1982) *J. Polym. Sci.: Polym. Chem. Ed.*, 20: 3207–3217.
6. Heatley, F., Lovell, P.A., and McDonald, J. (1993) *Eur. Polym. J*, 29: 255–268.
7. Matsumoto, A., Asai, S., and Aota, H. (2000) *Macromol. Chem. Phys*, 201: 2735–2741.
8. Paris, R. and de la Fuente, J.L. (2004) *J. Polym. Sci.: Part A: Polym. Chem.*, 43: 2395–2406.
9. Mennicken, M., Nagelsdiek, R., Keul, H., and Höcker, H. (2004) *Macromol. Chem. Phys.*, 205: 2429–2437.
10. Nagelsdiek, R., Mennicken, M., Maier, B., Keul, H., and Höcker, H. (2004) *Macromolecules*, 37: 8923–8932.
11. Hirano, T., Kitayama, T., Cao, J., and Hatada, K. (2000) *Polym. J*, 32 (11): 961–969.
12. Zulfigar, S., Masud, K., Piracha, A., and McNeill, I.C. (1997) *Polym. Degrad. Stab.*, 55: 257–263.
13. Zulfigar, S., Piracha, A., and Masud, K. (1996) *Polym. Degrad. Stab.*, 52: 89–93.
14. Zulfigar, S. and Masud, K. (2002) *Polym. Degrad. Stab.*, 78: 305–313.
15. Vardareli, T.K., Keskin, S., and Usanmaz, A. In press.